Letters in Applied NanoBioScience
Open-Access Journal (ISSN: 2284-6808)

Article
Volume 14, Issue 1, 2025, 6
https://doi.org/10.33263/LIANBS141.006

Antioxidant and Antidiabetic Activities of Triclisia Subcordata Oliv.: Experimental and Computational Methods

Akingbolabo Daniel Ogunlakin [1,2,*], Oluwafemi Adeleke Ojo [1,2], Dhamodharan Prabhu [3], Great Oluwamayokun Adebodun [4], Peluola Olujide Ayeni [2], Abayomi Samuel Adebodun [5], Mubo Adeola Sonibare [5], Omolola Adenike Ajayi-Odoko [6], Damilare IyinKristi Ayokunle [7]

1 Bowen University SDG 03 (Good Health and Wellbeing Research Cluster), Nigeria
2 Phytomedicine, Molecular Toxicology, and Computational Biochemistry Research Laboratory (PMTCB-RL), Department of Biochemistry, Bowen University, Iwo, 232101, Nigeria
3 Center for Drug Discovery, Department of Biotechnology, Karpagam Academy of Higher Education, Coimbatore 641021, India
4 Department of Physiology, Babcock University, Ilesan Remo, Nigeria
5 Department of Pharmacognosy, Faculty of Pharmacy, University of Ibadan, Ibadan, Nigeria
6 Microbiology Programme, Bowen University, Iwo, 232101, Nigeria
7 Pure and Applied Biology Programme, Bowen University, Iwo, 232101, Nigeria
* Correspondence: gbolaogunlakin@gmail.com;

Scopus Author ID 57219326317
Received: 26.09.2023; Accepted: 7.07.2024; Published: 21.09.2024

Abstract: Diabetes mellitus (DM), a non-communicable disease, describes a metabolic condition with multiple etiology, including oxidative stress. Methanol extract of *Triclisia subcordata* leaf was subjected to *in vitro* antioxidant assays and antidiabetic assays. The phytoconstituents revealed through GC-MS analysis were docked against the target proteins α-amylase and α-glucosidase. The FRAP and OH radical scavenging activity results confirmed the antioxidant property of this plant, as shown by the DPPH inhibitory assay, which shows that the extract has a ferric-reducing antioxidant property. The methanol extract of *Triclisia subcordata* had a similar nitric oxide inhibitory activity with the standard ascorbic acid. The plant extract had high α-amylase inhibitory ability with low α-glucosidase inhibitory ability compared to the standard Acarbose. GC-MS analysis revealed 1,19-Eicosadiene,1,9-Tetradecadiene,3-Octyne,6-methyl, tetratetracontane, carbonic acid, and prop-1-en-2-yl tetradecyl ester in *T. subcordata* extract. In both the phytochemical bound complexes, the residues involved in the interaction with aspidospermidin-17-ol, 1-acetyl-19,21-epoxy-15,16-dimethoxy- has shown no major fluctuations, thus indicating that the phytochemical binding is stable during the simulation. The results of the study demonstrated that the enzymes α-amylase and α-glucosidase could be inhibited by 1 aspidospermidin-17-ol, 1-acetyl-19,21-epoxy-15,16-dimethoxy-, discovered by GC-MS analysis. It is advised that more research be done to determine *T. subcordata*'s harmful effects on nonhuman subjects.

Keywords: Diabetes mellitus; *Triclisia subcordata*; antioxidant; α-amylase; α-glucosidase.

1. Introduction

Diabetes mellitus (DM), a non-communicable disease, describes a metabolic condition with multiple etiology categorized by prolonged increase in the blood sugar level with disturbances of carbohydrate, fat, and protein metabolism. Diabetes could be a result of defects

in insulin secretion (non-availability of insulin in the body system), insulin action (inability of the available insulin to locate and bind to the insulin receptors), or both [1]. According to Greco and Hall [2], it is estimated that by 2045, approximately 700 million people worldwide will have type two diabetes mellitus. Also, half of diabetes deaths occur in people under the age of 70 years, and almost 80% of diabetes deaths occur in low and middle-income countries [3,4]. Nigeria has been reported with the highest burden of diabetes in Africa, with almost 4.2 million cases, followed by South Africa with about 2.6 million cases, Ethiopia with 1.9 million, and Tanzania with 1.7 million. About two million of the cases of diabetes are undiagnosed in Nigeria, and deaths associated with diabetes in Nigeria in 2013 were estimated to be 105,091 cases [5-8]. Oputa and Chineye [6] also reported that up to 73% of diabetes patients in Nigeria do not practice self-monitoring of blood glucose. Hence, this lack of sensitization and awareness increases the chance of high mortality caused by diabetes mellitus in the country.

Type 1 diabetes is a temporary rise in the body's blood sugar as a result of the non-availability of insulin hormone, while Type 2 is more severe. Type 2 Diabetes mellitus is a health condition where the insulin hormone is available but is not able to bind to the active site of the glucose because of the conformational reorganization that has taken place on the active site of the glucose; hence, there is a prolonged rise in the blood glucose level [7, 9]. At the same time, gestational diabetes describes a health disorder where there is a short-term upward shoot in the blood glucose level in pregnant women. To date, scientists are searching for reproducible ways of managing this disease, which poses a greater threat to the survival of humans.

Oxidative stress has been associated with the pathology of many diseases, which comprise atherosclerosis, neurodegenerative diseases such as Alzheimer's disease, cancer, diabetes mellitus, and inflammatory diseases, including psychiatric disorders or the aging process [9]. Free radicals are small transportable molecules that are highly reactive because of their unpaired electron. Free radicals were initially thought to be radicals with oxygen nuclei called reactive oxygen species (ROS); however, they also include a subgroup of reactive nitrogen species (RNS) and are all a product of normal cellular metabolism [10]. In order to regulate the excessive production of these free radicals and to create a balance, organisms have built protective systems and mechanisms against their toxic effects [11]. An antioxidant is a molecule stable enough to donate an electron to a rampaging free radical and neutralize its capacity to damage [12]. These antioxidants mainly delay or inhibit cellular damage through their free radical scavenging property [13]. Cells produce defense against excessive free radicals through their preventative mechanisms, repair mechanisms, physical defenses, and antioxidant defenses [14]. Antioxidants exist both in enzymatic and non-enzymatic forms in the intracellular and extracellular environment [15]. Antioxidants can be grouped into two classes: synthetic and natural antioxidants [16]. The difference between the two categories is that most synthetic antioxidants generate substances that develop cancer or other diseases [17]. The body produces different antioxidants (endogenous) to neutralize free radicals and protect the body from different diseases caused by tissue injury. Exogenous antioxidants, which are externally supplied to the body through food, also play an important role in protecting the body [14, 18].

Triclisia subcordata Oliv. is a climbing shrub in the family Menispermaceae. It is a flowering plant of about 1.6 m long. It is locally known as Kanranjongbon and Alugboran among Yorubas in Southwestern Nigeria [19]. Abo *et al.* [20] and Odukoya *et al*. [21] reported

the pharmacological usage of this plant as an anti-inflammation herb. It is also used in the treatment of gout and internal wound [22,23]. *In silico* pharmacology and bioavailability study on *Triclisia subcordata* constituents proposed its antidiabetic property [24]. Therefore, this study investigated the antioxidant and antidiabetic potentials of *Triclisia subcordata* leaf.

2. Materials and Methods

2.1. Plant collection and extraction.

In June 2017, dirt-free leaves of *T. subcordata* were collected from the wild forest at Amina Way, University of Ibadan, Ibadan, Nigeria. The plant was identified and authenticated at the Forest Herbarium Ibadan (FHI), where it was given the voucher number FHI 110974. With random stirring, methanol was used to extract dried and pulverized *T. subcordata* leaves at room temperature for 72 hours. The extract was filtered, and the filtrate was concentrated in a rotary evaporator *in vacuo* at 37 ℃ (Buchi Rotavapour R-210, Switzerland). The extracted material was stored in the refrigerator for later use.

2.2. In vitro antioxidant assay.

2.2.1. 2,2-Diphenyl-1-picrylhydrazyl (DPPH) scavenging ability.

The free radical scavenging ability of the phenolics against DPPH free radicals was evaluated as described by Ogunlakin *et al*. [25]. An appropriate dilution of the phenolics (1 mL) was briefly mixed with 1 mL of 0.4 mM DPPH radicals in a methanolic solution. The mixture was left in the dark for 30 min, and the absorbance was taken at 516 nm. The control was carried out using 2 mL DPPH solution without the test samples. The DPPH free radical scavenging ability was subsequently as a percentage of the control.

2.2.2. Ferric reducing antioxidant power (FRAP) potential.

The reducing properties of the phenolics were determined by assessing the ability of the phenolics to reduce $FeCl_3$ solution, as described by Ogunlakin *et al*. [25]. A 2.5 mL aliquot was mixed with 2.5 mL of 200 mM sodium phosphate buffer (pH 6.6) and 2.5 mL of 1% potassium ferricyanide. The mixture was incubated at 50℃ for 20 min, and then 2.5 mL of 10% trichloroacetic acid was added. This mixture was centrifuged at 801 × *g* for 10 min. 5 mL of the supernatant was mixed with an equal volume of water and 1 mL of 0.1% ferric chloride. The absorbance was measured at 700 nm, and ferric reducing power was subsequently calculated using ascorbic acid equivalent.

2.2.3. Fenton's reaction (OH Radical scavenging activity).

The ability of the phenolics to prevent Fe^{2+}/H_2O_2-induced decomposition of deoxyribose was carried out using the method of Ogunlakin *et al*. [25]. Briefly, appropriate dilution of the phenolics was added to a reaction mixture containing 120 µL 20 mM deoxyribose, 400 µL 0.1M phosphate buffer, 40 µL 20 mM hydrogen peroxide, and 40 µL 500 µM $FeSO_4$, and the volume was made up to 800 µL with distilled water. The reaction mixture was incubated at 37℃ for 30 min, and the reaction was then stopped by the addition of 0.5 mL of 2.8% trichloroacetic acid (TCA); this was followed by the addition of 0.4 mL of 0.6% thiobarbituric acid (TBA) solution. The tubes were subsequently incubated in boiling water for

20 min. The absorbance was measured at 532 nm in a spectrophotometer. The percentage (%)˙OH radical scavenging ability was subsequently calculated.

2.2.4. Determination of Fe^{2+} chelating ability.

The Fe^{2+} chelating ability of both phenolics was determined using a modified method of Minotti and Aust [26], with a slight modification by Güven *et al*. [27]. Freshly prepared 500 µM $FeSO_4$ (150 µL) was added to a reaction mixture containing 168 µL of 0.1 M Tris-HCl (pH 7.4), 218 µL saline and the extracts (0 – 25 µL). The reaction mixture was incubated for 5 min before the addition of 13 µL of 0.25% 1,10-phenanthroline (w/v). The absorbance was subsequently measured at 510 nm in a spectrophotometer. The Fe^{2+} chelating ability was subsequently calculated.

2.2.5. Nitric oxide scavenging activity.

Nitric oxide scavenging assay was performed using the Griess reagent method, as reported by Lee *et al*. [28]. Briefly, 0.3 mL of sodium nitroprusside (5 mM) was added to 1 mL of each of the various concentrations of the extract. The test tubes were then incubated at 25℃ for 150 min. After 150 min, 0.5 mL of Griess reagent (equal volume of 1% sulphanilamide on 5% ortho-phosphoric acid and 0.01% naphthyl ethylenediamine in distilled water, used after 12hrs of preparation) was added. The absorbance was measured at 546 nm.

2.3. In vitro antidiabetic assays.

2.3.1. α-amylase inhibition assay.

This was measured using the dinitrosalicylic acid method described by Zulfiqar *et al*. [29]. Appropriate dilution of the flavonoid compounds (500 µL) and 500 µL of 0.02 M sodium phosphate buffer (pH 6.9 with 0.006 M NaCl) containing pancreatic α-amylase (EC 3.2.1.1) (0.5 mg/mL) were incubated at 25℃ for 10 min. Then, 500 µL of 1 % starch solution in 0.02 M sodium phosphate buffer (pH 6.9 with 0.006 M NaCl) was added to each tube. The reaction mixture was incubated at 25 ℃ for 10 min and stopped with 1.0 mL of dinitrosalicylic acid color reagent. Thereafter, the mixture was incubated in a boiling water bath for 5 min and cooled to room temperature. The reaction mixture was then diluted by adding 10 mL of distilled water, and absorbance was measured at 540 nm. The compounds' IC_{50} (the flavonoid compound concentration inhibiting 50% of the α-amylase activity) was calculated.

2.3.2. α-glucosidase inhibition assay.

Appropriate dilution of the flavonoid compounds (50 µL) and 100 µL of α-glucosidase solution (1.0 U/mL) in 0.1 M phosphate buffer (pH 6.9) were incubated at 25℃ for 10 min. Then, 50 µL of 5 mM p-nitrophenyl-α-D-glucopyranoside solution was added in 0.1 M phosphate buffer (pH 6.9). The mixtures were incubated at 25℃ for 5 min before reading the absorbance at 405 nm in the spectrophotometer [30]. The α-glucosidase inhibitory activity was expressed as percentage inhibition. The compounds' IC_{50} (the flavonoid compound concentration inhibiting 50 % of the α-glucosidase activity) was calculated.

2.4. Gas chromatography-mass spectrometry analysis.

The methanol extract was analyzed using an Agilent Technologies 7890 gas chromatography apparatus and an Agilent Technologies 5975 mass spectrometer. The HP5MS column is 30 meters long, 0.320 millimeters in diameter internally, and 0.25 milliliters thick. The temperature inside the oven increases to 240℃ after 6 minutes, from 80 ℃, which is maintained for 2 minutes at a rate of 12 ℃ each minute. The temperature of the sample was 250℃ when it was introduced into the GC/MS interface. The scan spans from 50 to 500 and uses splitless analysis [9].

2.5. Molecular docking.

2.5.1. Preparation of receptor and ligand molecules for molecular docking.

The three-dimensional structure of the target proteins α-amylase and α-glucosidase were retrieved from the macromolecule structure repository – RCSB Protein DataBank using the PDB ID: 4W93 and 5NN8, respectively. Schrodinger Protein Preparation Wizard was used to prepare the three-dimensional structures of the target proteins by altering the bond orders, adding hydrogen atoms, forming zero-order bonds to metal atoms, establishing disulfide bonds, and generating het states (PPW). The phytochemicals identified from the MS analysis were used as the ligands, and the structures of the ligands were retrieved from the PubChem database (Pubchem). All the 14 molecules collection were prepared using the LigPrep module of Schrodinger, where phytochemical structural variations were developed by assigning proper charges and bond orders. Further, the phytochemicals were optimized using OPLS3e force field (Ligprep). EPIK minimizations generated the phytochemicals' protonation states, and the phytochemicals' chirality combinations were retained during the tautomer generated. A maximum of 32 possible conformations were developed for the phytochemicals in the ligand preparation process.

2.5.2. Molecular docking of phytochemicals.

The protein structures were initially optimized with minimized hydrogen atoms, and further, the structure was minimized using the OPLS3e force field. The co-crystalized inhibitor molecules were retained during the protein preparation process to facilitate the receptor grid generation. Using the default parameters, the grid around the substrate molecule binding site was created using Schrodinger's "receptor grid generation" tool using the OPLS3e force field (Grid). The prepared phytochemicals were docked using the Schrodinger Glide XP module, which precisely docks the molecules into the defined binding site of the α-amylase and α-glucosidase proteins. Glide XP computes the binding energy and affinity of the phytochemicals with the highest precision and accuracy. The docking program utilizes glide scoring functions to rank the phytochemicals based on the XP score (Glide).

2.5.3. Molecular dynamics simulation studies (MDS) of protein-ligand complexes.

The ligand-bound α-amylase and α-glucosidase complexes were solvated in the orthorhombic-shaped boxes with single-point charge water molecules using the System Builder tool in Desmond v7.2. The counter ions and 0.15 M NaCl salt concentration were maintained to neutralize the systems during the α-amylase and α-glucosidase complexes simulations. Both

the ligand-bound complexes were individually simulated for 200ns using an OPLS forcefield in Desmond v7.2. Desmond's eight-stage default relaxation protocol and steepest descent minimization were applied prior to the production of MD simulations. During the simulations, 1 atm pressure and 300 K temperature were maintained using the isotropic Martyna–Tobias–Klein barostat and the Nose–Hoover thermostat, respectively. The smooth particle mesh Ewald method was used to analyze long-range coulombic interactions, and 9.0 was set as the short-range cutoff. Using an r-RESPA integrator, nonbonded forces were calculated, and every step was for short-range forces, and every three steps were periodically used for the long-range forces. The Simulation Interaction Diagram tool included in the Desmond MD package was used to analyze the behavior and interactions between the ligand and protein.

2.6. Statistical analysis.

The data was analyzed using software called GraphPad Prism version 9.0.1. We reported descriptive statistics as mean ± SD. GraphPad was used to analyze the results, which are presented as graphs. To compare the means, a statistical method known as one-way ANOVA was followed by Tukey's post hoc test with a significance level of $p < 0.05$.

3. Results and Discussion

3.1. In vitro antioxidant activity.

Reactive oxygen species (ROS) and free radicals are involved in the etiology of various health disorders such as cardiovascular and metabolic diseases, diabetes, and cancer due to the inability of antioxidants to manage the excess ROS [31,32]. An imbalance between free radicals production and the activities of antioxidants results in oxidative stress, which can cause damaged cellular proteins, DNA, membrane lipids, and eventually cell death [32]. Reducing oxidative stress could effectively manage many diseases, including diabetes and metabolic disorders [33]. Phytochemicals like phenolic compounds and flavonoids derived from plants have antioxidant potential and effectively manage and treat several diseases [34,35]. The quality and concentration of these phytochemicals are directly proportional to the antioxidant activities of plants [36]. DPPH, ABTS, FRAP, and metal chelating assays are used to identify the presence of antioxidants [37,38]. DPPH, a stable free radical, analyses antioxidants' free radical scavenging potentials by accepting hydrogen radicals and electrons from antioxidant molecules [31, 38]. The % DPPH scavenging ability of the methanol extract of *Triclisia subcordata* was highest at 0.04 mg/mL, showing that the antioxidant ability is dose-dependent (Figure 1). This is in comparison with the standard Ascorbic acid. In the FRAP assay, the antioxidants and ferric tripyridyltriazine complex react, resulting in blue-colored ferrous tripyridyltriazine [36]. Increased FRAP value indicates a higher antioxidant potential [38].

The FRAP and OH radical scavenging activity results confirmed the antioxidant property of this plant, as shown by DPPH (Figures 2 and 3), and this shows that the extract has a ferric-reducing antioxidant property. Flavonoids and phenolics decrease the formation of free radicals and also scavenge free radicals [34]. Iron, a metal ion, promotes lipid peroxidation via the Fenton reaction, and its chelating ability lowers the concentration of the transition metal involved in catalyzing lipid peroxidation [39]. The ion-chelating ability of the methanol extract of *Triclisia subcordata* increased as the concentration increased, suggesting that the Fe^{2+} chelation of the extract is dose-dependent (Figure 4). The extract's radical scavenging and ion-

chelating properties can be attributed to the presence of alkaloids, terpenoids, and polysaccharides [40, 41]. Thus, the plant extract can be considered an effective free radical scavenger, which is supported by the study by Akinwunmi *et al*. [42].

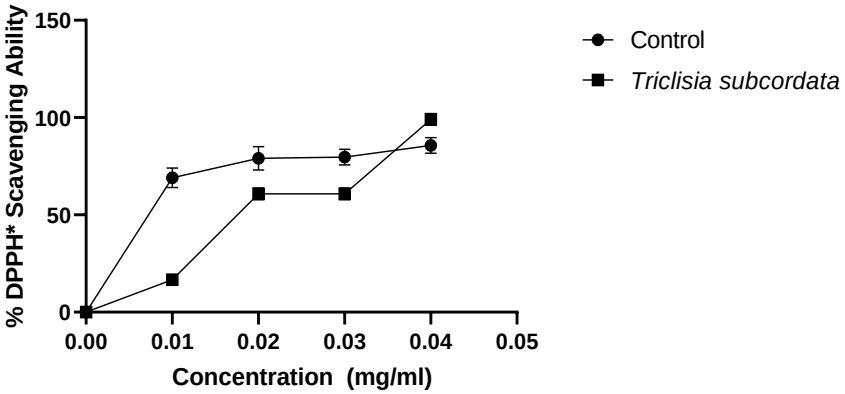

Figure 1. DPPH radical scavenging ability of *T. subcordata* leaves**.**
Data are represented as mean ± SD (n = 3). Control = ascorbic acid.

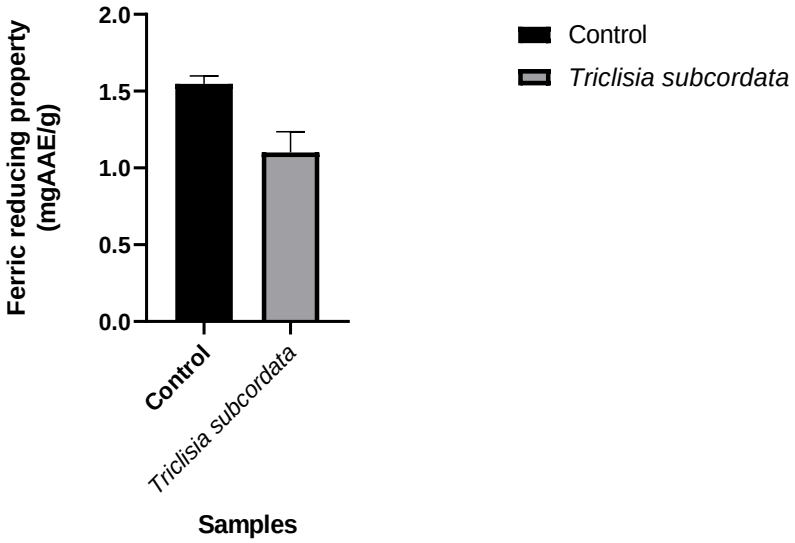

Figure 2. Ferric reducing antioxidant power of *T. subcordata* leaves.
Data are represented as mean ± SD (n = 3). Control = ascorbic acid.

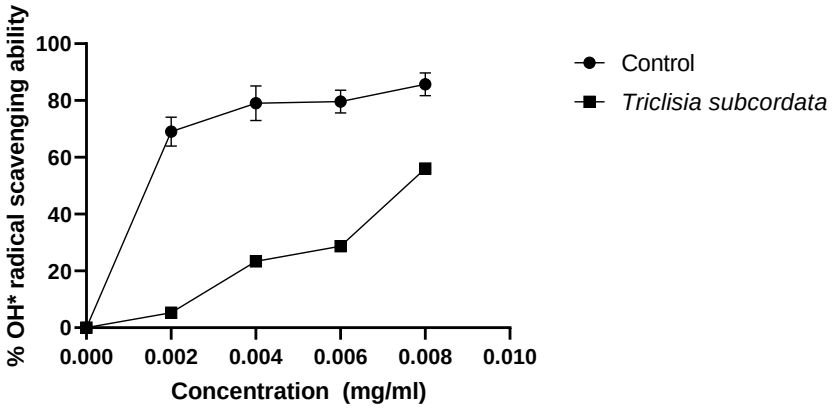

Figure 3. OH radical scavenging ability of *T. subcordata* leaves.
Data are represented as mean ± SD (n = 3). Control = ascorbic acid.

Methanol extract has been discovered to possess better antioxidant properties than other non-polar solvents. This could be attributed to the presence of flavonoids and the polarity of the active components [43, 44]. Nitric oxide is implicated in diabetes, inflammation, and cancer. The *in vitro* NO assay measures the breakdown of nitrate and nitrite. The methanol extract of *Triclisia subcordata* had a similar nitric oxide inhibitory activity with the standard ascorbic acid (Figure 5), suggesting that the extract is an excellent nitric oxide scavenger.

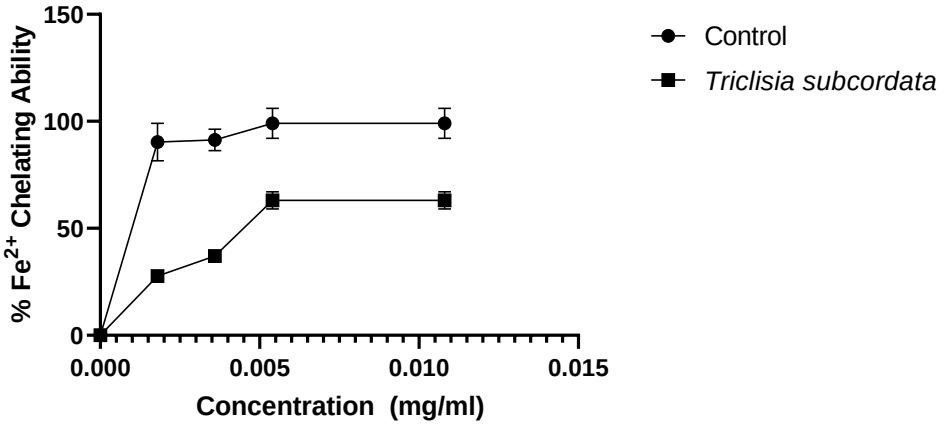

Figure 4. Fe^{2+} chelating ability of *T. subcordata* leaves.
Data are represented as mean ± SD (n = 3). Control = ascorbic acid.

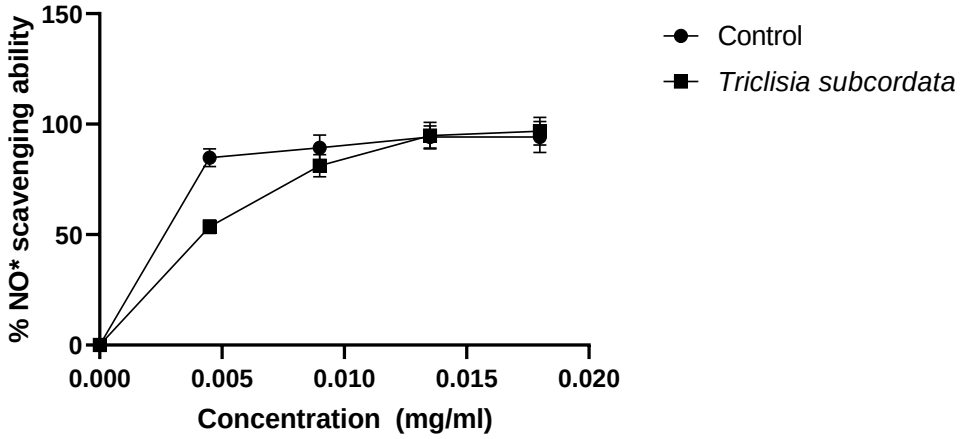

Figure 5. NO* Scavenging ability of *T. subcordata* leaves.
Data are represented as mean ± SD (n = 3). Control = ascorbic acid.

3.2. In vitro antidiabetic activity.

The antidiabetic potential of plants is evaluated by testing their ability to inhibit α-glucosidase and α-amylase, which are carbohydrate-hydrolyzing enzymes. α-amylase lowers the rate of starch conversion to glucose, thereby preventing increased blood glucose after food consumption [45]. *In vitro* inhibition of α-glucosidase and α-amylase by methanol extract of *Triclisia subcordata* was investigated. In this study, the plant extract had high α-amylase inhibitory ability with low α-glucosidase inhibitory ability compared to the standard (Figures 6 and 7). A dose-dependent α-amylase inhibition was observed in the methanol extract, with 0.03 and 0.04 mg/mL exhibiting the maximum inhibition. Low α-amylase and α-glucosidase inhibitory potential was also reported in both methanol and dichloromethane extracts of *Triclisia subcordata* by Akinwunmi *et al*. [42].

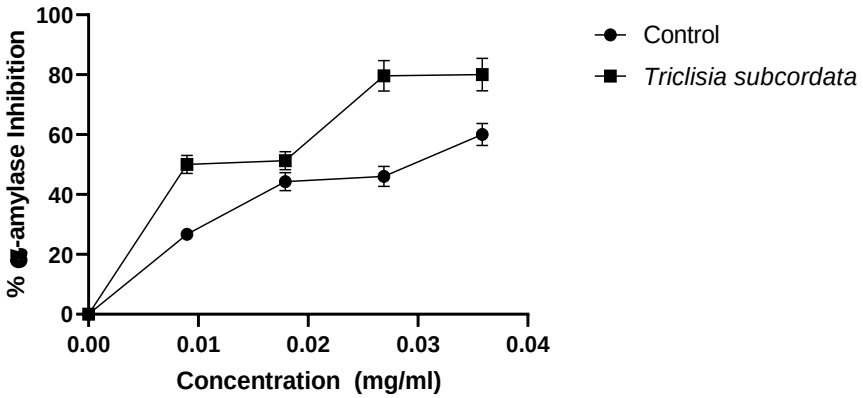

Figure 6. α-amylase inhibitory effect of *T. subcordata* leaves.
Data are represented as mean ± SD (n = 3). Control = Acarbose.

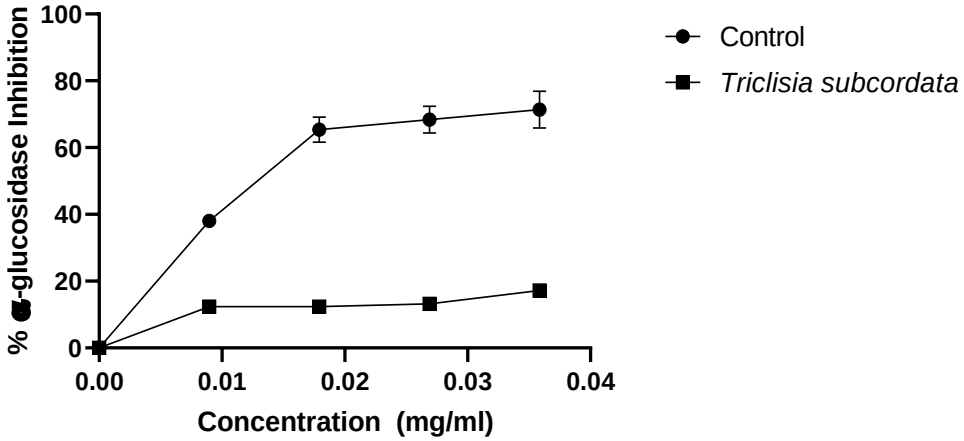

Figure 7. α-glucosidase inhibitory effect of *T. subcordata* leaves.
Data are represented as mean ± SD (n = 3). Control = Acarbose.

3.3. GC-MS analysis.

The GC-MS has been proven to be the most effective method of identifying various components present in plants [46].

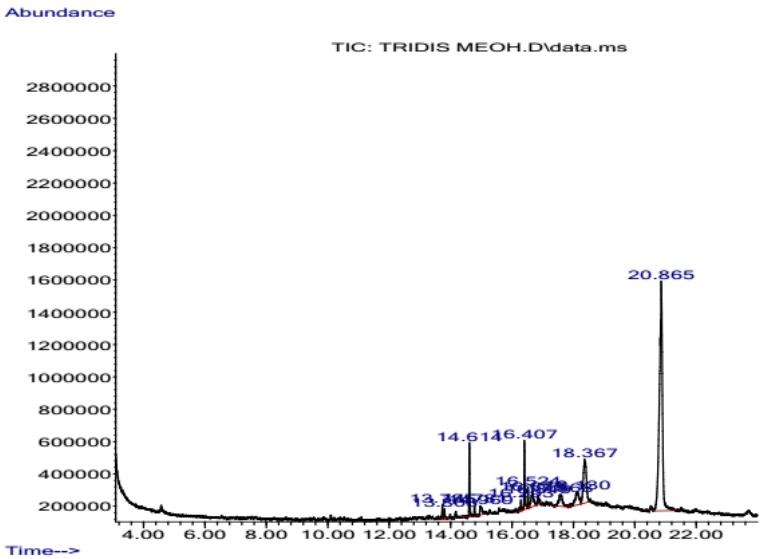

Figure 8. GC-MS chromatogram of *T. subcordata* leaves methanol extract.

The phytochemical compounds were identified by retention time and peak area. A total of 14 compounds were identified by GC-MS analysis in the *Triclisia subcordata* extract, these active components, the peak area and retention time are presented in Table 1. 1,19-Eicosadiene,1,9-Tetradecadiene,3-Octyne,6-methyl had the least retention time of 13.734 mins while Tetratetracontane, Carbonic acid, prop-1-en-2-yl tetradecyl ester had the highest retention time 20.863 mins (Table 1, Figure 8).

Table 1. Phyto-constituents of *T. subcordata* leaves detected via GCMS analysis.

Compounds Name	Area (%)	RT
1,19-Eicosadiene, 1,9-Tetradecadiene, 3-Octyne, 6-methyl-	1.10	13.734
13-Methyltetradecanal, 7-Oxabicyclo[4.1.0]heptane, 3-methyl-1-Hexadecanol, 2-methyl-,1-Hexadecanol, 2-methyl-	0.75	13.801
Pentadecanoic acid, 14-methyl-, methyl ester, Hexadecanoic acid, methyl ester,	4.35	14.616
2-Methyl-Z,Z-3,13-octadecadienol, 1,9-Tetradecadiene, 2(1H)-Benzocyclooctenone, decahydro-4a-methyl-, trans-(-)	0.77	14.782
9-Oxabicyclo[6.1.0]nonane, cis-, 9-Oxabicyclo[6.1.0]nonane, Tridecanedial	1.70	14.969
2(1H)-Naphthalenone, octahydro-, trans-, 12-Methyl-E,E-2,13-octadecadien-1-ol, 8-Dodecenol	0.97	16.292
1,2-Epoxyundecane, Phytol, Carbonic acid, 2-ethylhexyl heptadecyl ester	5.01	16.406
Methyl 8,10-dimethyl-hexadecanoate or 8,10-dimethyl-16:0, Methyl 11-oxo-9-undecenoate, 13,16-Octadecadiynoic acid, methyl ester	1.36	16.526
Cyclohexene, 4-(4-ethylcyclohexyl) -1-pentyl-, Undec-10-ynoic acid, undecyl ester, 3-Octyne, 6-methyl-	3.44	16.676
13-Tetradece-11-yn-1-ol, 1,6-Cyclodecadiene, Ethyl 9.cis.,11.trans.-octadecadienoate	0.55	16.847
Octadecane, 1-(ethenyloxy)-, Oxalic acid, isobutyl pentadecyl ester, Aspidospermidin-17-ol, 1-acetyl-19,21-epoxy-15,16-dimethoxy-	4.03	17.568
4-Pentenal, 2-methylene-, 3,8-Dioxatricyclo[5.1.0.0(2,4)]octane, 4-ethenyl-, 2-Pentyn-1-ol	4.67	18.129
Farnesol formate, trans-Sesquisabinene hydrate, trans-Farnesol	11.59	18.368
Tetratetracontane, Carbonic acid, prop-1-en-2-yl tetradecyl ester	59.70	20.863

3.4. In silico antidiabetic effect.

3.4.1. Molecular docking of phytochemicals with α-amylase and α-glucosidase.

The molecular docking results of 17 phytochemicals into the binding cavity of α-amylase and α-glucosidase are shown in Table 1. Among the 17 phytochemicals, Aspidospermidin-17-ol, 1-acetyl-19,21-epoxy-15,16-dimethoxy- has produced higher glide XP score of -6.285 kcal/mol and -4.958 kcal/mol with the Glide energy of -35.428 kcal/mol and -35.195 kcal/mol for α-amylase and α-glucosidase, respectively. The Aspidospermidin-17-ol, 1-acetyl-19,21-epoxy-15,16-dimethoxy- binding within the cavity of the α-amylase is stabilized by three hydrogen bonds (Figure 9a). The amino acid Asp197 has formed a hydrogen bond (CO---HO) at a distance of 2.31Å with the phytochemical. Where the uncharged polar amino acid Gln233 has formed a hydrogen bond (OH---OH) with the phytochemical at a distance of 1.94 Å. The positively charged His299 has established an NH---OC hydrogen bond at a distance of 2.11 Å with the phytochemical. All three hydrogen bonds mediated between the phytochemical and receptor protein α-amylase are less than 2.5Å. In general, the hydrogen bonds formed within 2.5Å are referred to as strong hydrogen bonds and, in turn, depict the strong binding of the phytochemical within the cavity of the α-amylase. While under the semi-flexible docking conditions, Aspidospermidin-17-ol, 1-acetyl-19,21-epoxy-15,16-dimethoxy- binding into the cavity of α-glucosidase was stabilized by a salt bridge (CO—NH) at the

distance of 4.08Å (Figure 9b). In order to understand the stability of the bound phytochemical under a real-time biological environment, the docked complexes were further taken to perform molecular dynamics simulations.

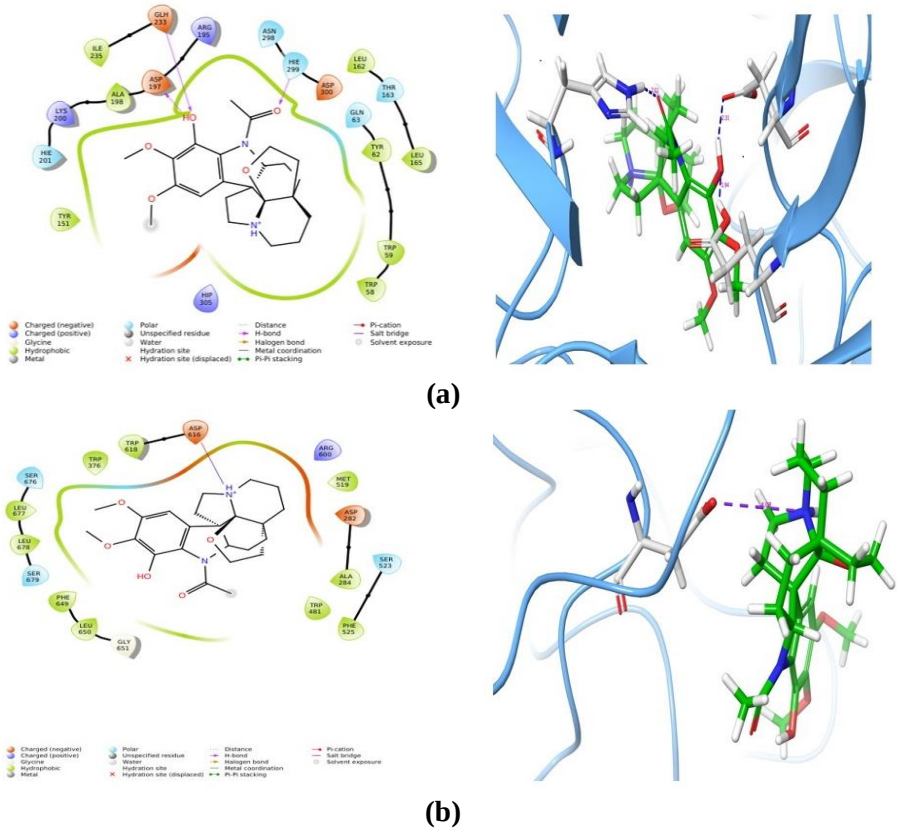

(a)

(b)

Figure 9. The 2D and 3D interaction profile of phytochemical with **(a)** α-amylase; **(b)** α-glucosidase.

3.4.2. Molecular dynamics simulation of phytochemical bound with α-amylase and α-glucosidase complexes.

The 200 ns molecular dynamics simulation trajectories were analyzed to evaluate the binding stability of the Aspidospermidin-17-ol, 1-acetyl-19,21-epoxy-15,16-dimethoxy- within the binding site of the receptor proteins. The average variation in the displacement of a particular set of atoms for a particular frame relative to a reference frame is calculated using the root mean square deviation (RMSD). All protein frames are first aligned based on the reference backbone structure prior to computing the atom-wise RMSD. The conformation changes in the protein structure during the simulation were monitored using the RMSD graphs. The RMSD graph of the phytochemical bound α-amylase complex depicted that the system attained equilibrium quickly, and the RMSD of the complex stabilized around 1.8Å (Figure 10a).

Similarly, the RMSD graph of the phytochemical bound α-glucosidase complex indicates that the average RMSD is 1.95Å, and the system has attained equilibrium within 25 ns of the timeframe (Figure 10b). However, at the depth of the simulation timeframe, the system has started adjusting the conformations, which leads to an increase in the RMSD. The RMSD deviations up to 3Å are acceptable for the small and globular proteins, while the deviation higher than 3Å depicts the protein undergoing significant structural and conformational changes during the simulation. The average RMSD of the phytochemical bound α-amylase and

α-glucosidase complexes were lesser than 2Å; the binding of the phytochemical is observed to be stable during the simulation timeframe.

The individual amino acid level fluctuations along the protein during the simulations were characterized using the Root Mean Square Fluctuation (RMSF). The RMSF graphs depict the individual amino acid fluctuations, in which the peak corresponds to the higher fluctuation of the corresponding amino acids in the simulated timeframe. The average C-alpha RMS fluctuation of the phytochemical bound α-amylase and α-glucosidase complexes were 0.95Å and 0.91Å, respectively (Figures 11a and 11b). Among the residues of α-amylase, non-polar side chain amino acids Gly351 and uncharged polar amino acid Asn350 have shown higher fluctuation more than 4Å (4.91Å and 4.75Å, respectively. Moreover, four nonpolar amino acids Gly365, Gly460, Gly306, and Gly144 have fluctuated more than 3Å, such as 3.51Å, 3.51Å, 3.47Å, and 3.04Å. Meanwhile, the uncharged polar residues Asn364, Asn459, and Asn352 indicated residual fluctuations up to 3.86Å, 3.74Å, and 3.59Å. In addition, the amino acids Gln349 and Phe348 registered fluctuations to the scale of 3.28Å and 3.43Å. Though few amino acids have shown RMS fluctuations between 3.0Å and 4.91Å, predominant residues have shown RMS fluctuations less than 1Å. Similarly, the case of α-glucosidase has depicted that 12 amino acids fluctuated between the scale of 5.90Å and 3.01Å. The α-glucosidase, a large protein complex compared to α-amylase, has indicated 5.90Å and 5.32Å fluctuations for Gln115 and Ala204. Only one uncharged polar amino acid, Gln81, the N-terminal residues registered fluctuations up to 4.16Å. Whereas, other nine amino acids such Glu795, Pro205, Ser679, Glu453, Ala452, Pro681, Lys114, Leu678 and Glu145 has indicated the fluctuations between 3.98Å and 3.01Å.

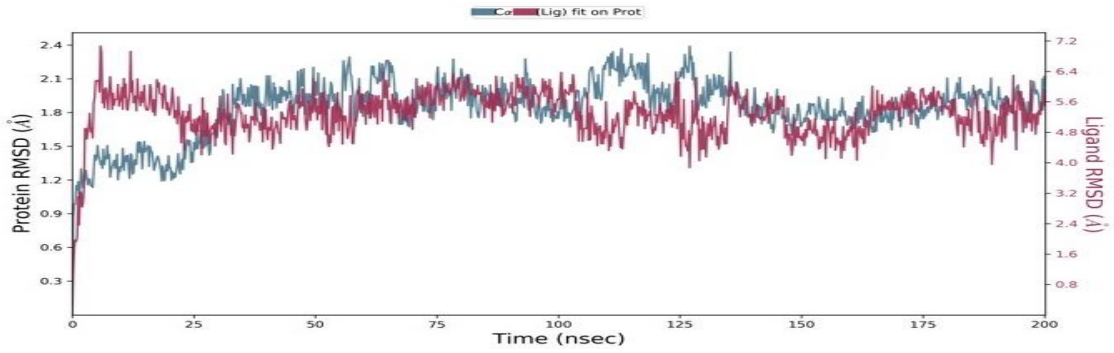

(a)

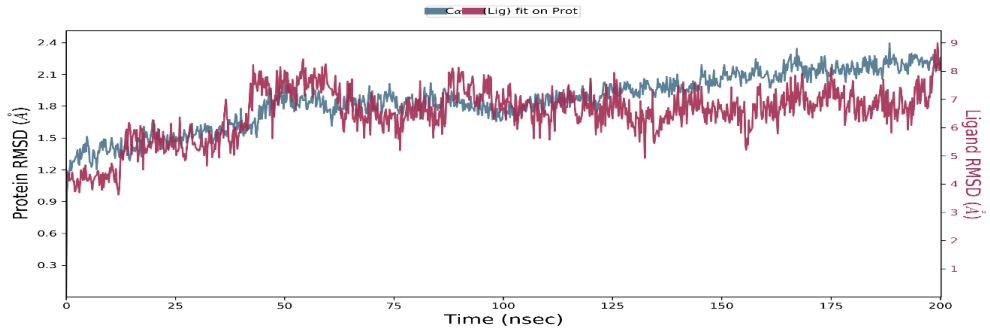

(b)

Figure 10. Root mean square deviations of the receptor protein C-alpha and ligand RMSD. **(a)** α-amylase; **(b)** α-glucosidase.

In both the phytochemical bound complexes, the residues involved in the interaction with Aspidospermidin-17-ol, 1-acetyl-19,21-epoxy-15,16-dimethoxy- has shown no major

fluctuations, thus indicating that the phytochemical binding is stable during the simulation. In general, the RMS fluctuations less than 3Å are considered stable movement, and thus, the bound phytochemical has influenced the integral binding within the enzyme. The N-and-C-terminal tail residues are more loosely bound than other integral core structures of the protein and tend to fluctuate more during the simulations. Also, the rigid secondary structural parts such as helices and sheets have less tendency to move or fluctuate during the simulation, while the unstructured portions or free loops often fluctuate in higher order during the simulation and in the real-time environment.

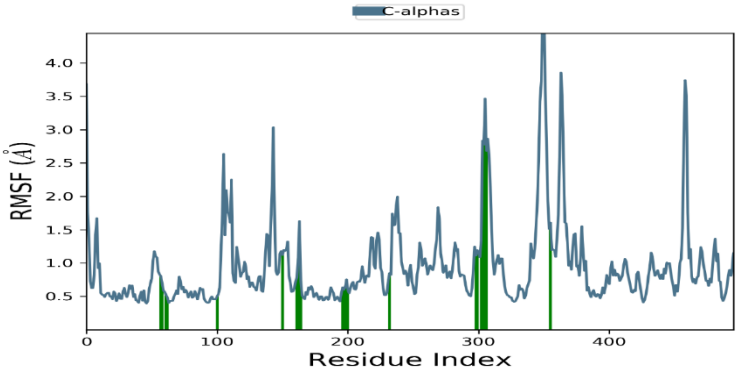

(a)

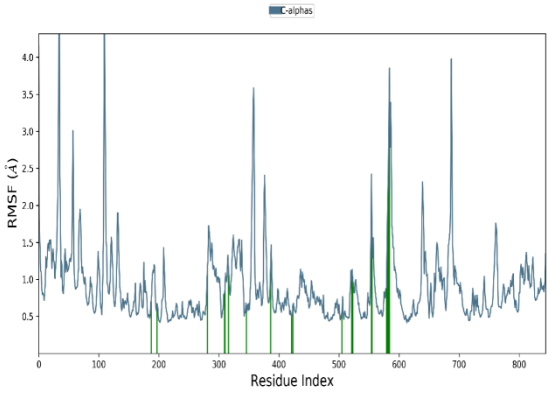

(b)

Figure 11. Root mean square fluctuations of the receptor protein C-alpha **(a)** α-amylase; **(b)** α-glucosidase.

3.4.3. Receptor–phytochemical interaction analysis.

The trajectories analysis of Aspidospermidin-17-ol, 1-acetyl-19,21-epoxy-15,16-dimethoxy- bound α-amylase and α-glucosidase simulations revealed four types of interactions, which stabilize the binding of the phytochemical molecule within the receptor active site cavities. The Aspidospermidin-17-ol, 1-acetyl-19,21-epoxy-15,16-dimethoxy- has established 22 interactions with α-amylase (Figure 12a), which comprises three hydrogen bonds (Gln63, His101, Asp197), seven hydrophobic interactions (Trp58, Trp59, Tyr62, Leu162, Leu165, Ala198, and His305), one ionic contact (His305), and 11water bridges (Tyr62, His101, Tyr151, Thr163, Asp197, Lys200, His299, Asp300, His305, and Asp356). An interaction fraction value of 0.7 or higher indicates that the particular contact is maintained for around 70% of the simulation duration. As some protein residues may make several interactions of the same subtype with the ligand, values higher than 1.0 are feasible. Among these 22 interactions, only three residues, namely, Gln63 (hydrogen bond: 0.98), Trp59 (hydrophobic: 1), and Asp197 (water bridge: 0.98), have been predominantly involved in the prime stabilization of the

Aspidospermidin-17-ol, 1-acetyl-19,21-epoxy-15,16-dimethoxy- within the cavity of α-amylase. Similarly, the phytochemical has formed 28 interactions with α-glucosidase (Figure 12b), in which two hydrogen bonds (Asp404, and Trp481), nine hydrophobic contacts (Trp376, Leu405, Arg411, Ile441, Trp481, Trp516, Phe649, Leu677, and Leu678), six ionic interactions (Asp282, Tyr292, Asp404, Trp481, Asp518, and Asp616), and 11 water bridges (Asp282, Trp376, Arg411, Trp481, Arg600, Asp616, Trp618, His674, Ser676, Leu677 and Leu678). Among these 28 interactions, only the Trp376 (hydrophobic interaction fraction value: 0.75) and hydrogen bond mediated by Asp404 (fraction value: 0.83) have an interaction fraction value higher than 0.7. This interaction analysis depicts that the aspidospermidin-17-ol, 1-acetyl-19,21-epoxy-15,16-dimethoxy- has been stably bound within the cavity during simulations, which in turn may have the potential inhibitory properties.

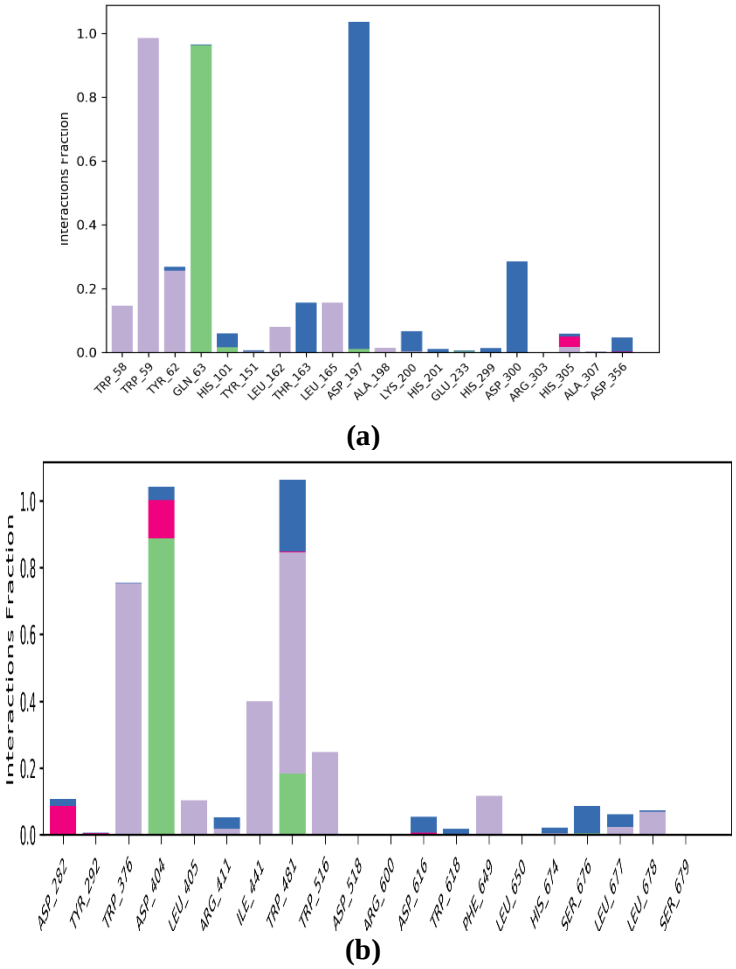

Figure 12. Protein-ligand interaction analysis. The histogram chart shows the various types of interactions mediated between the ligand and receptor protein **(a)** α-amylase; **(b)** α-glucosidase. Blue: Water bridges, Green: Hydrogen bonds, Pink: Ionic interactions, and Purple: Hydrophobic.

4. Conclusions

The results of this investigation showed that *T. subcordata* leaf contains a sizable amount of secondary metabolites, which are probably in charge of the plant's antioxidant and antidiabetic properties. This study's findings were further corroborated by the discovery that the bioactive compounds discovered by GC-MS have antioxidant and diabetic properties. The results of the study demonstrated that the enzymes α-amylase and α-glucosidase can be

inhibited by Aspidospermidin-17-ol, 1-acetyl-19,21-epoxy-15,16-dimethoxy-. It is advised that more research be done to determine *T. subcordata*'s harmful effects on nonhuman subjects.

Funding

This research received no external funding.

Acknowledgments

We acknowledged all staff members of the Biochemistry program at Bowen University, Iwo, for their support.

Conflicts of Interest

The authors declare no conflict of interest.

References

1. Petersen, M.C.; Shulman, G.I. Mechanisms of Insulin Action and Insulin Resistance. *Physiol. Rev*. **2018**, *98*, 2133-2223, https://doi.org/10.1152/physrev.00063.2017.
2. Greco, C.W.; Hall, J.M. Diabetic Kidney Disease: Goals for Management, Prevention, and Awareness. *Encyclopedia* **2023**, *3*, 1145-1156, https://doi.org/10.3390/encyclopedia3030083.
3. Azadnajafabad, S.; Ahmadi, N.; Rezaei, N.; Rashidi, M.-M.; Saeedi Moghaddam, S.; Mohammadi, E.; Abbasi-Kangevari, M.; Naderian, M.; Ghasemi, E.; Farzi, Y.; Kazemi, A.; Dilmaghani-Marand, A.; Yoosefi, M.; Rezaei, S.; Nasserinejad, M.; Fattahi, N.; Rezaei, N.; Haghshenas, R.; Foroutan Mehr, E.; Koolaji, S.; Razi, F.; Djalalinia, S.; Larijani, B.; Farzadfar, F. Evaluation of the diabetes care cascade and compliance with WHO global coverage targets in Iran based on STEPS survey 2021. *Sci. Rep.* **2023**, *13*, 13528, https://doi.org/10.1038/s41598-023-39433-7.
4. World Health Organization 2010, Fact sheet on Diabetes Mellitus. https://www.who.int/health-topics/diabetes# (accessed on 12 December **2022**).
5. Olatidoye, O.P. Diabetic Care Center and Nutrition/Dietetics in Nigeria. In Medical Entrepreneurship: Trends and Prospects in the Digital Age, Raimi, L., Oreagba, I.A., Eds.; Springer Nature Singapore: Singapore, **2023**; 287-310, https://doi.org/10.1007/978-981-19-6696-5_19.
6. Oputa, R.N.; Chinenye, S. Diabetes in Nigeria – a translational medicine approach. *Afr. J. Diabetes Med.* **2015**, *13*, 7-10.
7. Dahiru, T.; Aliyu, A.A.; Shehu, A.U. A Review of Population-based Studies on Diabetes Mellitus in Nigeria. S. Afr. Med. J. **2016**, *3*, 59-64, https://doi.org/10.4103/2384-5147.184351.
8. World Health Organisation. Definition, Diagnosis and Classification of Diabetes Mellitus and its Complications Report of a WHO Consultation, 1999 (accessed on 12 December **2022**).
9. Ogunlakin, A.D.; Ojo, O.A.; Gyebi, G.A.; Akinwumi, I.A.; Adebodun, G.O.; Ayokunle, D.I.; Ambali, O.A.; Ayeni, P.O.; Awosola, O.E.; Babatunde, D.E.; Akintunde, E.A.; Ajayi-Odoko, O.A.; Dahunsi, O.S.; Sonibare, M.A. Elemental evaluation, nutritional analysis, GC-MS analysis and ameliorative effects of *Artocarpus communis* J.R.Forst. & G.Forst. seeds' phytoconstituents on metabolic syndrome via *in silico* approach. *J. Biomol. Struct. Dyn.* **2023**, 1-21, https://doi.org/10.1080/07391102.2023.2293271.
10. Obeagu, E.I. A Review on Free Radicals and Antioxidants. Int. J. Curr. Res. Med. Sci. **2018**, *4*, 123-133.
11. Laher, I. Systems Biology of Free Radicals and Antioxidants; Springer Canada, **2014**.
12. Lobo, V.; Patil, A.; Phatak, A.; Chandra, N. Free Radicals, Antioxidants and Functional Foods: Impact on Human Health. *Pharmacogn. Rev.* **2010**, *4*, 118, https://doi.org/10.4103/0973-7847.70902.
13. Halliwell, B. How to characterize an antioxidant: an update. *Biochem. Soc. Symp.* **1995**, *61*, 73-101, https://doi.org/10.1042/bss0610073.
14. Mahantesh, S.P.; Gangawane, A.K.; Patil, C.S. Free radicals, antioxidants, diseases and phytomedicines in human health: future perspects. *World Res. J. Med. Aromat. Plant.* **2012**, *1*, 6–10.
15. Nimse, S.B.; Pal, D. Free radicals, natural antioxidants, and their reaction mechanisms. *RSC Adv.* **2015**, *5*, 27986–28006, https://doi.org/10.1039/C4RA13315C.

16. Butnariu, M.; Grozea, L. Antioxidant (Antiradical) Compounds. *J. Bioequivalence Bioavailab.* **2012**, *4*, 17-19, https://doi.org/10.4172/jbb.10000e18.
17. Giacalone, M.; Di Sacco, F.; Traupe, I.; Topini, R.; Forfori, F.; Giunta, F. Antioxidant and neuroprotective properties of blueberry polyphenols: a critical review. *Nutr. Neurosci.* **2011**, *14*, 119–125, https://doi.org/10.1179/1476830511Y.0000000007.
18. Sun, Y.; Jin, D.; Zhang, Z.; Zhang, Y.; Zhang, Y.; Kang, X.; Jiang, L.; Tong, X.; Lian, F. Effects of antioxidants on diabetic kidney diseases: mechanistic interpretations and clinical assessment. *Chin. Med.* **2023**, *18*, 3, https://doi.org/10.1186/s13020-022-00700-w.
19. Sonibare, M.A.; Adebodun, S.A. Macroscopic and microscopic evaluation of *Triclisia subcordata* Oliv. (Menispermaceae) towards its standardization. Niger. J. Pharm. *Res.* **2018**, *14*, 189-196.
20. Abo, K.A.; Lawal, I.O.; Ogunkanmi, L.A. Evaluation of extracts of Triclisia suboardata Oliv and Heinsia crinita (Afz) G. Taylor for antimicrobial activity against some clinical bacterial isolates and fungi. Afr. J. Pharm. *Pharmacol.* **2011**, *5*, 125-131.
21. Odukoya, O.A.; Sofidiya, M.O.; Samuel, A.T.; Ajose, I.; Onalo, M.; Shuaib, B. Documentation of Wound Healing Plants in Lagos-Nigeria: Inhibition of Lipid Peroxidation as In-vivo Prognostic Biomarkers of Activity. *Ann. Biol. Res.* **2012**, *3*, 1683-1689
22. Sonibare, M.A.; Onifade, T.R.; Ogunlakin, A.D.; Akinmurele, O.J.; Adebodun, S.A. Microscopic evaluation and antioxidant activity of Glyphaea brevis (Spreng.) Monach.(Family Tiliaceae). *Free Radic. Antioxid.* **2022**, *12*, 27-32, https://doi.org/10.5530/fra.2022.1.5.
23. Popoola, O.K.; Adekeye, K.D.; Akinbinu, E.D.; Adekeye, L.T.; Afolayan, M.B.; Bakare, E.A.; Akande, O.E. Ethnobotanical plants and their tradomedicinal values: A review. World J. Biol. Pharm. Health Sci. **2021**, *5*, 066-088, https://doi.org/10.30574/wjbphs.2021.5.1.0108.
24. Ogunlakin, A.D.; Onifade, T.R.; Gyebi, G.A.; Obafemi, B.A.; Ojo, O.A. In silico pharmacology and bioavailability of bioactive constituents from Triclisia subcordata (Oliv), an underutilized medicinal plant in Nigeria. *Plant Sci. Today* **2023**, *10*, 260-268, https://doi.org/10.14719/pst.2292.
25. Ogunlakin, A.D.; Odugbemi, A.I.; Omolekan, T.; Adaramoye, O.A.; Abiola, O.O.; Akinola, A.; Akinsete, A.; Alabi, T.; Alade, F.F.; Ahossinme, H.E.; Ajiboye, A.; Ajiboye, T.A.; Ajila, O.; Ajisafe, T.L.; Sonaike, O.; Akinadewo, A.O.; Akinbiyi, T.A.; Olajide, T.J.; Oni, I.D.; Shittu, S.A.; Bakare, F.; Ojo, O.A. Elemental and *In vitro* Antioxidant Studies of Some *Bracharia* species and Milk from Bowen University Dairy Farm. *IOP Conf. Ser.: Earth Environ. Sci.* **2023**, *1219*, 012003, https://doi.org/10.1088/1755-1315/1219/1/012003.
26. Minotti, G.; Aust, S.D. An investigation into thee mechanism of citrate FE^{2+}-dependent lipid peroxidation. *Free Radic. Biol. Med.* **1987**, *3*, 379-387, https://doi.org/10.1016/0891-5849(87)90016-5.
27. Güven, L.; Erturk, A.; Miloğlu, F.D.; Alwasel, S.; Gulcin, İ. Screening of Antiglaucoma, Antidiabetic, Anti-Alzheimer, and Antioxidant Activities of *Astragalus alopecurus* Pall—Analysis of Phenolics Profiles by LC-MS/MS. *Pharmaceuticals* **2023**, *16*, 659, https://doi.org/10.3390/ph16050659.
28. Lee, Y.M.; Lee, S.; Kim, W.J. Nitric oxide scavengers based on *o*-phenylenediamine for the treatment of rheumatoid arthritis. *Biomater. Sci.* **2023**, *11*, 2395-2404, https://doi.org/10.1039/D2BM01994A.
29. Zulfiqar, S.; Blando, F.; Orfila, C.; Marshall, L.J.; Boesch, C. Chromogenic Assay Is More Efficient in Identifying α-Amylase Inhibitory Properties of Anthocyanin-Rich Samples When Compared to the 3,5-Dinitrosalicylic Acid (DNS) Assay. *Molecules* **2023**, *28*, 6399, https://doi.org/10.3390/molecules28176399.
30. Hu, C.-M.; Zheng, Y.-Y.; Lin, A.-T.; Zhang, X.; Wu, X.-Z.; Lin, J.; Xu, X.-T.; Xiong, Z. Design, synthesis and evaluation of indole-based bisacylhydrazone derivatives as α-glucosidase inhibitors. *J. Mol. Struct*. **2023**, *1271*, 134124, https://doi.org/10.1016/j.molstruc.2022.134124.
31. Sharma, S.; Padhi, S.; Chourasia, R.; Dey, S.; Patnaik, S.; Sahoo, D. Phytoconstituents from *Urtica dioica* (stinging nettle) of Sikkim Himalaya and their molecular docking interactions revealed their nutraceutical potential as α-amylase and α-glucosidase inhibitors. J. Food Sci. Technol. **2023**, *60*, 2649-2658, https://doi.org/10.1007/s13197-023-05789-x.
32. Arulselvan, P.; Fard, M.T.; Tan, W.S.; Gothai, S.; Fakurazi, S.; Norhaizan, M.E.; Kumar, S.S. Role of Antioxidants and Natural Products in Inflammation. *Oxid. Med. Cell. Longev.* **2016**, *2016*, 5276130, https://doi.org/10.1155/2016/5276130.
33. Singh, J.; Parasuraman, S.; Kathiresan, S. Antioxidant and antidiabetic activities of methanolic extract of Cinnamomum cassia. *Pharmacogn. Res.* **2018**, *10*, 237–242, http://dx.doi.org/10.4103/pr.pr_162_17.

34. Sonter, S.; Mishra, S.; Dwivedi, M.K.; Singh, P.K. Chemical profiling, in vitro antioxidant, membrane stabilizing and antimicrobial properties of wild growing *Murraya paniculata* from Amarkantak (M.P.). *Sci. Rep.* **2021**, *11*, 9691, https://doi.org/10.1038/s41598-021-87404-7.
35. Ogunlakin, A.D.; Sonibare, M.A. Ameliorative effect of *Kigelia africana* (Lam.) Benth. fruit methanol extract in letrozole-induced polycystic ovarian syndrome rat. Kuwait J. Sci. **2023**, *50*, 622-626, https://doi.org/10.1016/j.kjs.2023.05.018.
36. Liew, S.S.; Ho, W.Y.; Yeap, S.K.; Sharifudin, S.A.B. Phytochemical composition and in vitro antioxidant activities of *Citrus sinensis* peel extracts. *Peer J.* **2018**, *6*, e5331, https://doi.org/10.7717/peerj.5331.
37. Attar, U.A.; Ghane, S.G. *In vitro* antioxidant, antidiabetic, antiacetylcholine esterase, anticancer activities and RP-HPLC analysis of phenolics from the wild bottle gourd (*Lagenaria siceraria* (Molina) Standl.). S. Afr. J. Bot. **2019**, *125*, 360-370, https://doi.org/10.1016/j.sajb.2019.08.004.
38. Patel, S.B.; Attar, U.A.; Sakate, D.M.; Ghane, S.G. Efficient extraction of cucurbitacins from *Diplocyclos palmatus* (L.) C. Jeffrey: Optimization using response surface methodology, extraction methods and study of some important bioactivities. *Sci. Rep.* **2020**, *10*, 2109, https://doi.org/10.1038/s41598-020-58924-5.
39. Rabeta, M.S.; Nur Faraniza, R. Total phenolic content and ferric reducing antioxidant power of the leaves and fruits of *Garcinia atrovirdis* and *Cynometra cauliflora*. *Int. Food Res. J.* **2013**, *20*, 1691-1696.
40. Chandra Mohan, S.; Balamurugan, V.; Thiripura Salini, S.; Rekha, R. Metal ion chelating activity and hydrogen peroxide scavenging activity of medicinal plant *Kalanchoe pinnata*. *J. Chem. Pharm. Res.* **2012**, *4*, 197–202.
41. Vedamurthy, A.B.; Padmaa, M.P.; Sudisha, J. Antibacterial and antioxidant activities of fractionated persea *gratissim* seed extracts. *World J. Pharm. Pharm. Sci.* **2015**, *4*, 480–486.
42. Ogunlakin, A.D.; Awosola, O.E.; Ajayi, G.T.; Ojo, O.A. Review on Phytochemistry of Medicinal Plants Documented for the Treatment of Low Sperm Count in Oluponna, Nigeria. *Pharmacogn. J*. **2023**, *15*, 439-446, http://dx.doi.org/10.5530/pj.2023.15.69.
43. Akinwunmi, O.A.; Adekeye, D.K.; Olagboye, S.A. Phytochemical quantification, *in vitro* antioxidant and antidiabetic potentials of methanol and dichloromethane extracts of *Triclisia subcordata* (Oliv) leaves. Trends Phytochem. *Res.* **2020**, *4*, 17-24.
44. Sharma, V.; Janmeda, P. Extraction, isolation and identifcation of favonoid from *Euphorbia neriifolia* leaves. *Arab. J. Chem.* **2017**, *10*, 509–514, https://doi.org/10.1016/j.arabjc.2014.08.019.
45. Kartini, S.; Juariah, S.; Mardhiyani, D.; Bakar, M.F.A.; Bakar, F.I.A.; Endrini, S Phytochemical Properties, Antioxidant Activity and α- Amilase Inhibitory of Curcuma Caesia. *J. Adv. Res. Appl. Sci. Eng. Technol.* **2023**, *30*, 255–263, https://doi.org/10.37934/araset.30.1.255263.
46. Khan, A.; Pervaiz, A.; Ansari, B.; Ullah, R.; Shah, S.M.; Khan, H.; Saeed Jan, M.; Hussain, F.; Ijaz Khan, M.; Albadrani, G.M.; Altyar, A.E.; Abdel-Daim, M.M. Phytochemical Profiling, Anti-Inflammatory, Anti-Oxidant and In-Silico Approach of *Cornus macrophylla* Bioss (Bark). *Molecules* **2022**, *27*, 4081, https://doi.org/10.3390/molecules27134081.